Biol. Cybern. 58, 313–320 (1988)

Biological Cybernetics

White-Noise Analysis of Nonlinear Behavior in an Insect Sensory Neuron: Kernel and Cascade Approaches

M. J. Korenberg, A. S. French, and S.K.L. Voo

Department of Electrical Engineering, Queen's University, Kingston, Ontario, K7L 3N6 Canada and
Department of Physiology, University of Alberta, Edmonton, Alberta, T6G 2H7 Canada

Abstract. A functional expansion was used to model the relationship between a Gaussian white noise stimulus current and the resulting action potential output in the single sensory neuron of the cockroach femoral tactile spine. A new precise procedure was used to measure the kernels of the functional expansion. Very similar kernel estimates were obtained from separate sections of the data produced by the same neuron with the same input noise power level, although some small time-varying effects were detectable in moving through the data. Similar kernel estimates were measured using different input noise power levels for a given cell, or when comparing different cells under similar stimulus conditions. The kernels were used to identify a model for sensory encoding in the neuron, comprising a cascade of dynamic linear, static nonlinear, and dynamic linear elements. Only a single slice of the estimated experimental second-order kernel was used in identifying the cascade model. However, the complete second-order kernel of the cascade model closely resembled the estimated experimental kernel. Moreover, the model could closely predict the experimental action potential train obtained with novel white noise inputs.

1 Introduction

During the past 20 years white noise analysis techniques have been increasingly employed to model nonlinear dynamic biological systems, particularly in the field of neural information coding and processing (Marmarelis and Naka 1972; French and Wong 1977; Marmarelis and Marmarelis 1978; Sakuranaga et al. 1986). In their pioneering application of white noise analysis to the retina, Marmarelis and Naka (1972) used the Lee-Schetzen (1965) cross-correlation method of kernel estimation, following the functional expansion approach developed by Wiener (1958). They estimated the first- and second-order Wiener kernels of a three stage neural chain whose output consisted of action potentials. To obtain a continuous output signal they applied repeated sequences of an identical pseudo-random input signal and constructed a histogram of the output events. Subsequently, it was shown that repetition of the input was unnecessary and the kernels could be obtained by correlating the white Gaussian input directly with a unitized output signal, in which the output consisted of one, at the time of an action potential, and zero at all other times (Sakuranaga et al. 1987).

In practice, Wiener kernel analysis via the cross-correlation technique can result in inaccurate kernel estimates and poor system identification (Palm and Poggio 1978). This is partly due to the difficulty of experimentally realizing a white Gaussian input over an infinite time interval, as Wiener (1958) had assumed. Deviations from this ideal stimulation are inevitably caused by the frequency response and amplitude limitations of the physical systems used to apply the input, and the finite duration of real experiments.

To overcome these difficulties an exact orthogonal procedure was developed for estimating nonlinear system kernels (Korenberg et al. 1988). This procedure does not require the input to be white, Gaussian, or of infinite duration. Operating via Gram-Schmidt orthogonalization, the procedure creates, as an intermediate step, a series of functions which are orthogonal for the particular input and duration of the identification experiment. In this way, the procedure avoids a major source of error in the cross-correlation approach, and produces significantly more accurate kernel estimates.

However, it has subsequently become evident that the creation of orthogonal functions in this procedure is unnecessary and expensive in computing time and memory. Consequently, a newer fast orthogonal al-

gorithm was developed which can estimate kernels without the creation of orthogonal functions at any stage of the process (Korenberg 1987; 1988). This yields considerable efficiencies in time and memory requirements. Depending on the application, 15-fold or higher increases in speed are readily attainable without loss of accuracy or robustness. The newer technique allows small personal computers to deal with kernel sizes and data records which were previously difficult to analyse interactively on large mainframe computers with the usual memory restrictions.

Kernel estimation via the fast orthogonal algorithm has been shown to be much more accurate than the cross-correlation method using limited stimulus durations (Korenberg 1988). The superiority in accuracy was retained when the system output was corrupted with zero-mean stationary noise independent of the input. By eliminating the need for long data records the fast orthogonal algorithm makes it possible to analyse non-stationary systems by producing successive estimates of the kernels from brief data segments. As with the earlier orthogonal function method, the fast orthogonal algorithm does not require special autocorrelation properties of the input stimulus and is applicable to a variety of random and deterministic signals.

In this paper we present one of the first applications of the fast orthogonal algorithm to a biological system, the single sensory neuron in the cockroach femoral tactile spine. The kernels were used to construct a cascade model for the system, consisting of two dynamic linear elements separated by a static nonlinearity. Finally the cascade model was used to predict the unitized action potential output of the system to portions of the input stimulus which had not been used in the analysis.

2 Methods

2.1 The Experimental Preparation

The experimental procedures for stimulating and recording from the tactile spine neuron of the cockroach, *Periplaneta americana*, have been described in detail before (French 1984). Stimulation was provided by an extracellular electrode located adjacent to the soma-axon junction of the neuron and action potentials were detected by extracellular electrodes further along the axon. A pseudo-random binary sequence was generated from a 33-bit shift register clocked at 1 kHz (Marmarelis and Marmarelis 1978) and band-limited to 0–50 Hz by a nine-pole active filter. This noise signal was used to drive a constant voltage-to-current convertor which, in turn, stimulated the neuron. The stimulus current was monitored by a current detector in the ground return path and this signal was sampled by a 12-bit analog to digital convertor at 8 ms intervals. Action potentials were detected by a Schmitt trigger and fed to a digital input on the computer. The action potentials were used to construct a unitized output signal at 8 ms intervals consisting of values of 1, when an action potential had occurred within the interval, or 0 at all other times.

2.2 Analysis Procedures

Sections of the record containing 15,000 pairs of input values, $x(n)$, and output values, $y(n)$, were used for analysis. The relationship between the stimulating current and the unitized output was first approximated by a second-order discrete-time Volterra series (or functional expansion) of the standard form:

$$y_s(n)=h_0+\sum_{j=0}^{R-1} h(j)x(n-j) + \sum_{j_1=0}^{R-1}\sum_{j_2=0}^{R-1} h(j_1,j_2)x(n-j_1)x(n-j_2). \quad (1)$$

Here, the zero-, first-, and symmetric second-order kernels, h_0, $h(j)$, and $h(j_1,j_2)$ respectively, were selected to minimize the mean-square error:

$$e=\overline{(y(n)-y_s(n))^2}, \quad (2)$$

where the bar indicates a time average over the record length extending from $n=0$ to $n=N$. For a memory length $R=25$, one zero order, 25 first order and 325 distinct second order kernel values were estimated by the fast orthogonal algorithm.

The fast orthogonal algorithm may be understood by first considering the earlier orthogonal procedure (Korenberg et al. 1988). Estimating the kernels in (1) by direct least squares regression would lead to the solution of a large number of simultaneous linear equations in the unknown kernel values. For the memory length R in (1), one zero-order, R first-order, and $R(R+1)/2$ distinct second-order kernel values would be estimated simultaneously, requiring inversion of a square matrix having $1+R+R(R+1)/2$ columns. The earlier orthogonal procedure avoided this matrix inversion by rewriting (1) as a weighted sum of functions $W_i(n)$ orthogonal over the actual data record:

$$y_s(n)=\sum_{i=0}^{L} g_i W_i(n).$$

The $W_i(n)$ were constructed, via Gram-Schmidt orthogonalization, as linear combinations of the functions: 1, $x(n-j_1)$, $x(n-j_1)x(n-j_2)$; $j_1=0,\ldots,R-1$, $j_2=j_1,\ldots,R-1$. Since the $W_i(n)$ are mutually orthogonal, the weights g_i can be estimated independently of each other, avoiding the solution of simultaneous

equations. The mean square error in (2) is minimized when each weight is given by:

$$g_i = \overline{y(n)W_i(n)} / \overline{W_i^2(n)}.$$

It is then straightforward to convert these weights into the desired kernel values (Korenberg et al. 1988). While this orthogonal procedure does not require the input to be Gaussian or to have special autocorrelation properties, it is wasteful by explicitly creating the orthogonal functions as an intermediate step.

The fast orthogonal algorithm avoids creating the orthogonal functions by observing that they are only needed as parts of *time-averages*, for example in the above formula for the weights, g_i. In the original orthogonal procedure, Gram-Schmidt orthogonalization was used to define each $W_i(n)$ recursively in terms of previously created orthogonal functions. The fast orthogonal algorithm instead relates each time-average involving $W_i(n)$ to previously created time-averages. The first time average, involving $W_0(n)$ is easily calculated since $W_0(n) \equiv 1$ over the data record. The remaining time-averages are calculated recursively from the earlier ones, avoiding the creation of orthogonal functions. The only step-by-step averaging over each value of n required for kernel identification via the fast orthogonal algorithm is the calculation of input mean and autocorrelation, output mean, and cross-correlations with the input. These means and correlations are needed for the recursive formulas relating time averages involving $W_i(n)$ to time averages created previously. Major efficiencies in time and memory requirements ensue.

Since the input signal in this case closely resembled Gaussian white noise, the first- and second-order kernel estimates approximated the Wiener kernels of corresponding order. This enabled certain tests for cascade structure to be applied. For example, a discrete-time system having the Hammerstein model structure, comprising a static nonlinearity followed by a dynamic linear system, must satisfy the condition that:

$$h(j_1, j_2) = C_1 \delta(j_1 - j_2) h(j_1) \tag{3}$$

(Korenberg 1973a; Marmarelis and Marmarelis 1978; Hunter and Korenberg 1986) where C_1 is a constant and $\delta(j)$ is the discrete delta function. This implies that all non-diagonal values of the second-order kernel are zero, while diagonal values are proportional to the first-order kernel, provided that the latter is not identically zero.

A more general cascade model (Fig. 1) consists of a first dynamic linear system with delta response $g(j)$, a static nonlinearity $m(\cdot)$, and a second dynamic linear system with delta response $k(j)$. It can be shown (Korenberg 1985) that the delta response of the first linear system, $g(j)$, is proportional (for $j = 0, 1, \ldots$) to $h(j, 0)$, provided that the latter is not identically zero:

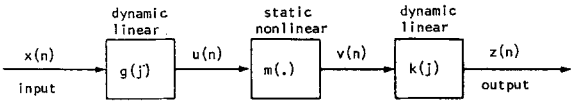

Fig. 1. The cascade model used to describe sensory encoding in the tactile spine. The three elements are a dynamic linear system, $g(j)$, a static nonlinearity, $m(\cdot)$, and a dynamic linear system, $k(j)$

$$g(j) = C_2 h(j, 0) \tag{4}$$

where C_2 is a constant. Moreover, the convolution of the two delta responses is proportional to $h(j)$, if $h(j) \not\equiv 0$:

$$\sum_{r=0}^{M} k(r) g(j-r) = C_3 h(j), \tag{5}$$

where C_3 is a constant and it is assumed that both $k(j)$ and $g(j)$ equal zero for $j > M$. Equations (4) and (5) can be solved to obtain $g(j)$ and $k(j)$ up to arbitrary proportionality constants and horizontal shifts. Since the proportionality, or scaling, constants are arbitrary, both C_2 and C_3 may be set equal to 1. Then, from (4) the delta response of the first linear system, $g(j)$, is given by one slice of the second-order Wiener kernel. With $g(j)$ and $h(j)$ known, (5) may be deconvolved to yield $k(j)$. Note that setting $j = 0, \ldots, M$ in (5) yields $M+1$ linear simultaneous equations in the unknowns $k(0), \ldots, k(M)$ which can readily be expressed in vector-matrix form. The coefficient matrix of this equation is nonsymmetric Toeplitz [a matrix is Toeplitz if the elements on any line parallel to the main diagonal are all equal; equivalently, all elements having the same row and column index difference are equal (Hunter and Kearney 1983)]. It is therefore possible to exploit a very efficient program for the solution of non-symmetric Toeplitz equations (Zohar 1979) and thereby obtain $k(j)$.

With $g(j)$ and $k(j)$ estimated it is immediately possible to test the necessary condition (Korenberg 1973a, b; Korenberg and Hunter 1986) for a system to have the cascade structure of Fig. 1:

$$h(j_1, j_2) = C_4 \sum_{r=0}^{M} k(r) g(j_1 - r) g(j_2 - r), \tag{6}$$

where C_4 is a constant. Note that this condition may be tested before estimating the static nonlinearity. Moreover, only the single slice $h(j, 0)$ of the second-order Wiener kernel was used in the above estimation of $g(j)$. Yet, if the system has the cascade structure of Fig. 1, we can use (6) to predict the shape of the complete second-order kernel, assuming it is not identically zero. In particular, we can predict the diagonal second-order kernel values $h(j, j)$, (up to a proportionality constant).

Assuming the necessary condition of (6) is satisfied, we can estimate a polynomial approximation for the static nonlinearity:

$$m(\cdot)=\sum_{i=0}^{I} a_i(\cdot)^i. \tag{7}$$

Suppose that $x(n)$ is defined for $n=0,\ldots,N$. Since $g(j)$ is known, compute:

$$u(n)=\sum_{j=0}^{\min(n,M)} g(j)x(n-j). \tag{8}$$

The output of the cascade is:

$$z(n)=\sum_{i=0}^{I} a_i \sum_{j=0}^{\min(n,M)} k(j)u^i(n-j). \tag{9}$$

We wish to choose the coefficients a_i to minimize the mean square error: $\overline{(y(n)-z(n))^2}$. To this end, we define for $n=0,\ldots,N$:

$$p_i(n)=\sum_{j=0}^{\min(n,M)} k(j)u^i(n-j), \quad i=0,\ldots,I. \tag{10}$$

Using Gram-Schmidt orthogonalization, set

$$\left.\begin{aligned} w_0(n)&=p_0(n)\\ w_i(n)&=p_i(n)-\sum_{r=0}^{i-1}\alpha_{ir}w_r(n), \quad i=1,\ldots,I, \end{aligned}\right\} \tag{11}$$

where

$$\alpha_{ir}=\overline{p_i(n)w_r(n)}/\overline{w_r^2(n)}. \tag{12}$$

The functions $w_i(n)$ in (11) are orthogonal over the record from $n=0$ to $n=N$, and (9) can be rewritten as an orthogonal series:

$$z(n)=\sum_{i=0}^{I} g_i w_i(n)$$

then:

$$g_i=\overline{y(n)w_i(n)}/\overline{w_i^2(n)}, \quad i=0,\ldots,I. \tag{13}$$

Finally, the desired coefficients a_i can be calculated from the following formula (Korenberg et al. 1988):

$$a_i=\sum_{m=i}^{I} g_m v_{m,i}$$

where

$$v_{i,i}=1$$

$$v_{m,i}=-\sum_{r=i}^{m-1}\alpha_{mr}v_{r,i}, \quad m=i+1,\ldots,I.$$

Note that the degree I of the polynomial estimate for the static nonlinearity can be considerably larger than 2, the assumed order of the Volterra series approximation (1) for the system. The reason is that the fast orthogonal algorithm yields least square estimates for the kernels in the functional series (1). Therefore, with a white Gaussian input, the first- and second-order kernel estimates will theoretically equal the Wiener kernels of corresponding order. This is true even if the system cannot be accurately approximated by a second-order Volterra series, as has been pointed out previously (Korenberg et al. 1988) for kernel estimates obtained by the earlier orthogonal procedure. Thus, the second-order functional series approximation suffices to yield the Wiener kernels, and hence determine the linear systems in the cascade, regardless of the degree of polynomial required for accurate expansion of the static nonlinearity. However, note that the mean square of each orthogonal function used in expanding the static nonlinearity must not be negligible. That is, (12) and (13) must not involve division by extremely small positive numbers, with resulting inaccuracies.

The identified cascade models were used to predict the unitized action potential output of the neural system in response to the white noise input. The raw output of the cascade already had a spike-like appearance, and a threshold level was set to convert this into a unitized signal. The threshold level was set to produce unitized data similar to the output during part of the record used for system identification. The same threshold was then used to predict the output but using parts of the record before or after the section which had been used for system identification.

3 Results

Figure 2 shows a second-order kernel estimate obtained from a tactile spine sensory neuron using the fast orthogonal algorithm. Since the current stimulus

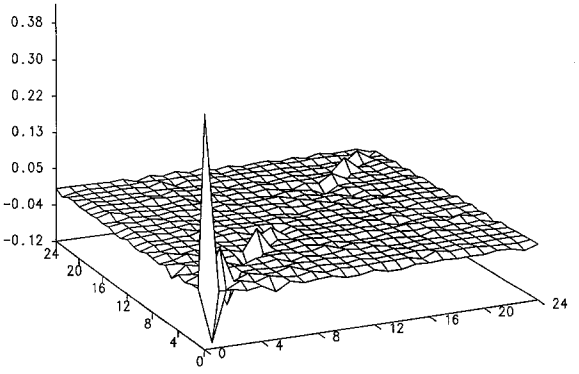

Fig. 2 Perspective plot of the second-order kernel, $h(j_1,j_2)$, obtained from 15,000 pairs of data points. The tactile spine neuron was stimulated with random noise having a bandwidth of 0–50 Hz and amplitude 4.47 nA rms. The lower two axes have the dimension of time in sample intervals of 8 ms, giving a total length of 192 ms in each case. The plot has been rotated through 25°. The same axes and rotation apply to all of the subsequent second-order plots. Note the sparcity of non-diagonal values

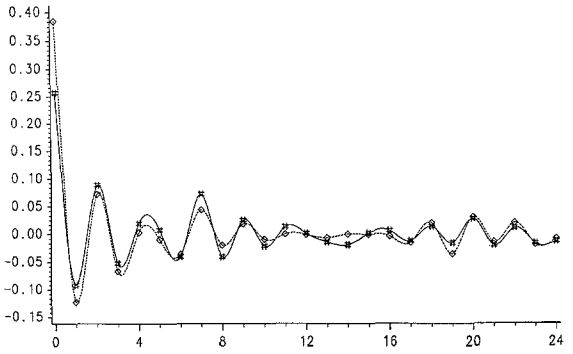

Fig. 3. The first-order kernel, $h(j)$, (solid lines) and the diagonal of the second-order kernel, $h(j,j)$, (dashed lines) for the same experiment as Fig. 2. The abscissa has the dimension of time in sample intervals of 8 ms, giving a total length of 192 ms. The same abscissa applies to all subsequent first-order plots. Note the excellent agreement over the entire lag time

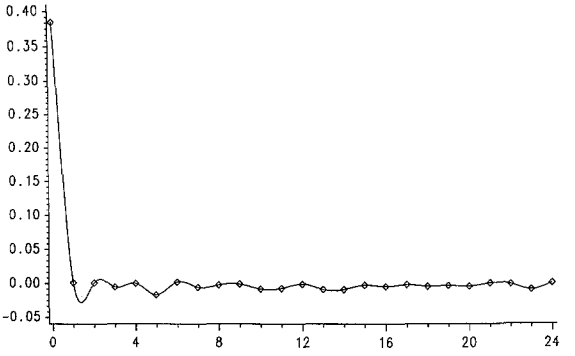

Fig. 4. The estimated first dynamic linear component of the cascade model, $g(j)$, obtained from the edge components $h(j,0)$ of the second-order kernel in Fig. 2. This curve, and all other linear plots, were fitted with a spline algorithm which accounts for the apparent dip between the second and third data points. In fact, all values other than the value at zero time are very close to zero in this case

approximated Gaussian white noise, and the system was best fit by a second-order Volterra series, the measured kernels approximate the first- and second-order Wiener kernels. The sparcity of off-diagonal kernel values in Fig. 2 suggests the possibility that the system could be accurately represented by the Hammerstein model, a necessary test for which is (3) (Hunter and Korenberg 1986). Accordingly, the first-order kernel estimated by the fast orthogonal algorithm was plotted together with the diagonal values of the second-order kernel estimate in Fig. 3. The two curves are in good agreement, even for long lag times, suggesting that the small variations in the tail of each curve, which might otherwise be dismissed as noise, may not be random, but actually characteristic of the sensory neuron. Note that such features would not be evident in cross-correlation estimates of the kernels because the inherent jitter and noise would mask such small variations.

We next estimated the components of the cascade model of Fig. 1. Figure 4 shows the estimate of $g(j)$ [obtained from $h(j,0)$], the delta response of the first linear system in the cascade. This response was negligible for lags greater than zero but significantly greater than zero for $j=0$. The dip in the plotted graph below zero for $1<j<2$ appears to be an artefact of the plotting routine, since the values at $j=1$ and $j=2$ are so close to zero. Sampling at higher resolution than the 8 ms used at present might reveal further structure in this delta response, but the data obtained here indicate that the first linear element is close to a discrete delta function, as is the case for the Hammerstein model.

Figure 5 shows the estimate of the second linear system in the cascade by deconvolution from the first-order kernel by the Toeplitz matrix method. The system appears to be band-pass and displays considerable ringing. Note that because the estimate of the first linear system was so close to a delta function, the delta response of the second linear system is similar to the first-order kernel estimate of Fig. 3.

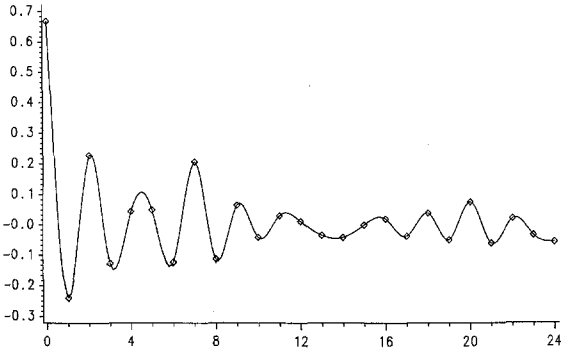

Fig. 5. The estimated second dynamic linear component of the cascade model, $k(j)$, obtained by deconvolving the first linear component from the first-order kernel of Fig. 3, using the Toeplitz matrix method. In contrast to the first linear component, this component has significant structure

A necessary condition for the system to be representable by a linear, static nonlinear, linear cascade model (Fig. 1) is given by (6). Figure 6 shows the second-order kernel synthesized using the right hand side of (6) with our estimates of $g(j)$ and $k(j)$. Except for an arbitrary scaling factor, there is excellent agreement between the synthesized second-order kernel and the experimental second-order kernel (Fig. 2) obtained via the fast orthogonal algorithm. It should be noted that only a single slice, $h(j,0)$, of the experimental second-order kernel was used to produce the synthesized second-order kernel.

The similarity between experimental and synthesized second-order kernels is further illustrated in

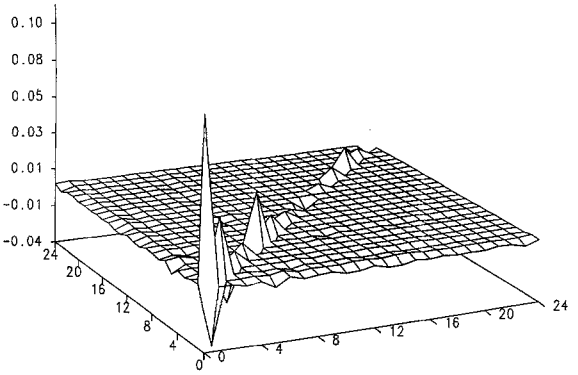

Fig. 6. The synthesized second-order kernel obtained from the two dynamic linear components, $g(j)$ and $k(j)$, in Figs. 4 and 5. Note the strong similarity to the experimental kernel of Fig. 2

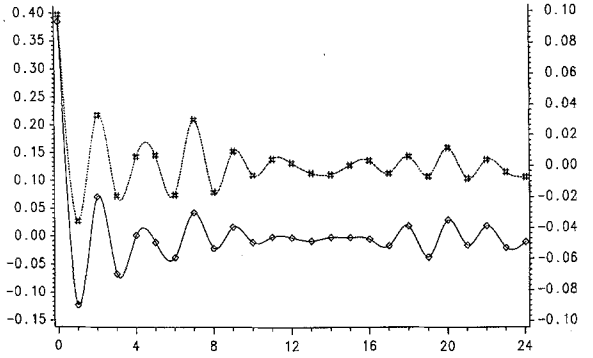

Fig. 7. The diagonal values of the synthesized second-order kernel of Fig. 6 (dashed line, right ordinate) compared with the diagonal of the experimental kernel of Fig. 2 (solid line, left ordinate). Again, there is close agreement between the predicted and experimental kernel values up to a proportionality constant

Fig. 7 by plotting the diagonal values of the kernels. In this figure the two curves have been deliberately shifted vertically to separate them, but the actual values of the curves are given on the left and right ordinates. Note that (6) is merely a necessary condition for a system to be representable by the cascade model of Fig. 1, but it is not a sufficient condition to ensure that the cascade model will represent the system accurately, even if the input is restricted to the present stimulus. A better test for the applicability of the cascade model is to predict the action potential output, and this was tested next.

Since the necessary condition for the cascade model was met satisfactorily, the form of the static nonlinearity was estimated to a fifth degree polynomial approximation and this is shown in Fig. 8. This function is quite similar to a half-wave rectifier, although in other experiments the rise of the function for strongly negative inputs to the static nonlinearity was more pronounced. The output of the complete cascade in response to the white noise input had

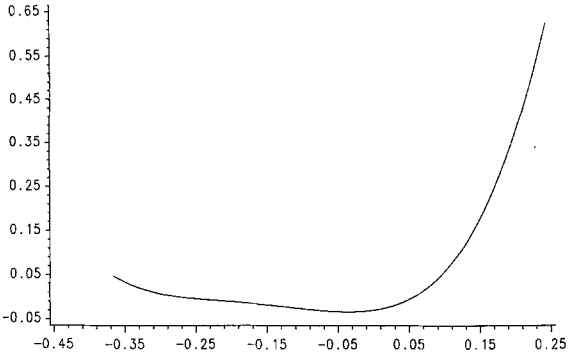

Fig. 8. The static nonlinear term in the cascade, $m(\cdot)$, as estimated by a fifth-order polynomial. Note the similarity to a half-wave rectifier, with the strong inflection at zero input

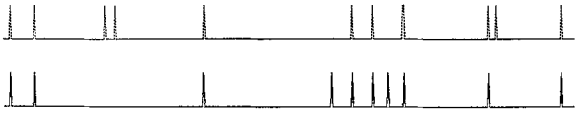

Fig. 9. The predicted output from the cascade model when stimulated with 500 data points from the original input and passed through a threshold to produce a unitized output signal. The solid lines are the actual unitized action potentials produced by the neuron in response to this input, and the dashed lines show the predicted output

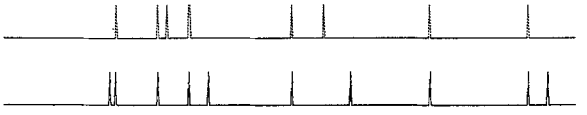

Fig. 10. The predicted output of the cascade model using the same threshold level as in Fig. 9, but with 500 input data points from the experimental record immediately before the data set used to identify the system. The actual response of the neuron is shown in solid lines and the predicted output in dashed lines

distinct positive peaks suggesting the appearance of action potentials. Using the middle 500 points of the input data used in the identification, we selected a threshold so that the output peaks produced a unitized signal conforming closely with the actual unitized record for the same input. The result of this operation is shown in Fig. 9, compared with the actual output of the sensory neuron. There is good agreement between the predicted and actual output signals but this might be expected since they were both produced from data used to identify the model and the threshold was chosen to enhance the similarity. As an independent test of the predictive ability of the cascade model we next performed the same operations using the same threshold and the 500 input data points immediately preceeding (Fig. 10) and immediately following

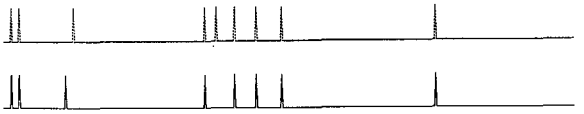

Fig. 11. The predicted output of the cascade model using the same threshold level as in Figs. 9 and 10, but with the 500 data points from the experimental record immediately after the data set used to identify the system. The actual output is in solid, the predicted output is dashed

(Fig. 11) the 15,000 points used in the identification. There is an obvious similarity between the unitized experimental data and the synthesized trains of action potentials, particularly in Fig. 11. This shows that the analytical technique applied here are sufficiently precise to produce mathematical models capable of accurately predicting the times of occurrence of individual action potentials in response to a random input.

Finally, Figs. 12, 13, and 14 show other second-order kernel estimates from experiments using 15,000 data points of white Gaussian noise input band-limited to 50 Hz. Figure 12 was obtained from an earlier segment of data for the same input power level (4.47 nA rms) stimulating the same neuron that was used for all of the previous figures. While there were some minor changes with time, the second-order kernel is clearly similar in amplitude and form to that from the later data shown in Fig. 2. The kernel in Fig. 13 was obtained from an experiment with the same neuron but with a higher amplitude stimulus of 23.91 nA rms. Some differences in form and a considerable difference in amplitude are evident although there is still a strong similarity to the kernel of Fig. 2. The second-order kernel of Fig. 14 was obtained from another tactile spine neuron using an input power level of 4.36 nA rms. Again there is strong similarity of form, though some difference in amplitude when compared to the earlier data in Fig. 2. In the present experiments we examined the behavior of 3 different tactile spine neurons in a total of ten different experiments at varying input power levels. In each case, nonlinear identification was performed for data segments near the start, middle, and end of experiments which typically lasted for 1 h. Similar and consistent shapes were obtained for the first- and second-order kernels in each of these experiments and good predictions were obtained for the output action potential trains to previously unused inputs.

4 Conclusions

The results obtained in these experiments provide strong support for the accuracy and reliability of the quantitative approach presented here. They also show

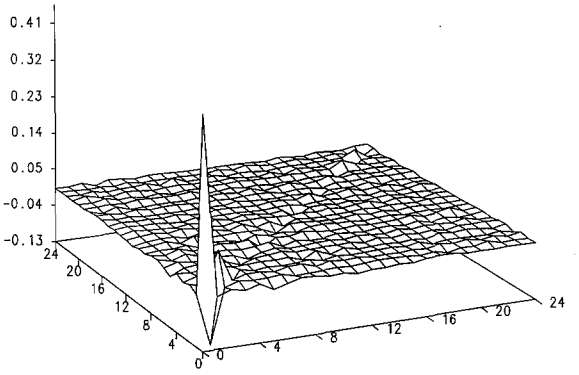

Fig. 12. The second-order kernel obtained by analysis of 15,000 data pairs from an earlier portion of the experiment which was used to obtain Fig. 2. The amplitude and form of the kernel are relatively stable with time during an experiment which lasted more than 1 h

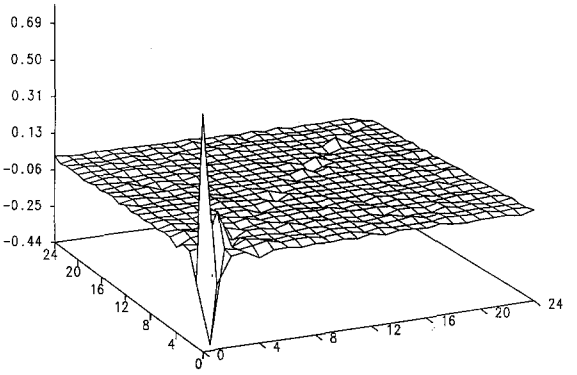

Fig. 13. The second-order kernel obtained by analysis of 15,000 data pairs from another experiment with the same neuron which was used in Figs. 2 and 12. In this case a much higher stimulus amplitude of 23.91 nA rms was used, producing a firing rate of about 13 action potentials per second, compared to a rate of about 2 action potentials per second in the earlier experiments. There is still a strong similarity between the estimated kernels

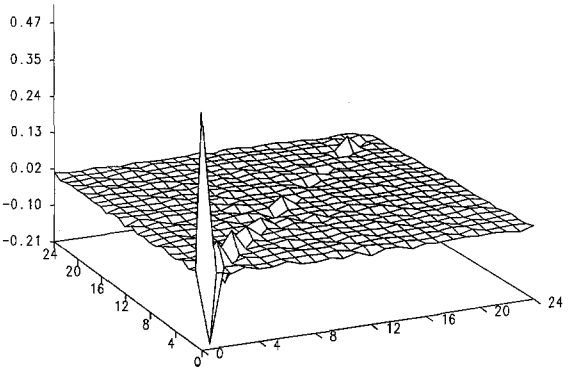

Fig. 14. The second-order kernel obtained from a different tactile spine neuron, using an input stimulus power of 4.36 nA rms and with an output of approximately 3 action potentials per second. Again, there is close agreement with the earlier second-order kernels

that the dynamic linear, static nonlinear, dynamic linear cascade model can provide reasonable predictions of the complete neural behavior. The estimated static nonlinearity (Fig. 8) closely resembles a half-wave rectifier. This agrees with the earlier suggestion by French (1980), based on first- and second-order kernel frequency response experiments, that the neuron displays half-wave rectification.

In future work we intend to apply this analysis technique to the behavior of other real and model neural encoders. In particular, an analysis of the Hodgkin-Huxley (1952) and related simulations offers the possibility of relating the forms of the estimated kernels to the detailed behavior of the ionic channels which provide the fundamental basis of neural encoding.

Acknowledgements. Expert technical assistance was provided by Rodney Gramlich. This work was supported by grants from the Medical Research Council of Canada, the Natural Sciences and Engineering Research Council of Canada, the Advisory Research Committee of Queen's University, and the Alberta Heritage Foundation for Medical Research.

References

French AS (1980) Sensory transduction in an insect mechanoreceptor: linear and nonlinear properties. Biol Cybern 38:115–123

French AS (1984) Action potential adaptation in the femoral tactile spine of the cockroach, *Periplaneta americana*. J Comp Physiol A 155:803–812

French AS, Wong RKS (1977) Nonlinear analysis of sensory transduction in an insect mechanoreceptor. Biol Cybern 26:231–240

Hodgkin AL, Huxley AF (1952) A quantitative description of membrane current and its application to conduction and excitation in nerve. J Physiol 117:500–544

Hunter IW, Kearney RE (1983) Two-sided linear filter identification. Med Biol Eng Comput 21:203–209

Hunter IW, Korenberg MJ (1986) The identification of nonlinear biological systems: Wiener and Hammerstein cascade models. Biol Cybern 55:135–144

Korenberg MJ (1973a) Identification of biological cascades of linear and static nonlinear systems. Proc Midwest Symp Circuit Theory 18.2:1–9

Korenberg MJ (1973b) Cross-correlation analysis of neural cascades. Proc Ann Rocky Mountain Bioeng Symp 1:47–52

Korenberg MJ (1985) Identifying noisy cascades of linear and static nonlinear systems. IFAC Symp Ident Sys Param Est 1:421–426

Korenberg MJ (1987) Functional expansions, parallel cascades and nonlinear difference equations. In: Marmarelis VZ (ed) Advanced methods of physiological system modelling. USC Biomedical Simulations Resource, vol 1. Los Angeles, pp 221–240

Korenberg MJ (1988) Identifying nonlinear difference equation and functional expansion representations: the fast orthogonal algorithm. Ann Biomed Eng (in press)

Korenberg MJ, Hunter IW (1986) The identification of nonlinear biological systems: LNL cascade models. Biol Cybern 55:125–134

Korenberg MJ, Bruder SB, McIlroy PJ (1988) Exact orthogonal kernel estimation from finite data records: extending Wiener's identification of nonlinear systems. Ann Biomed Eng (in press)

Lee YW, Schetzen M (1965) Measurement of the Wiener kernels of a nonlinear system by cross-correlation. Int J Control 2:237–254

Marmarelis PZ, Marmarelis VZ (1978) Analysis of physiological systems. The white noise approach. Plenum Press, New York

Marmarelis PZ, Naka K-I (1972) White noise analysis of a neuron chain: an application of the Wiener theory. Science 175:1276–1278

Palm G, Poggio T (1978) Stochastic identification methods for nonlinear systems: an extension of the Wiener theory. SIAM J Appl Math 34:524–534

Sakuranaga M, Ando Y-I, Naka K-I (1987) Dynamics of ganglion cell response in the catfish and dog retinas. I. Gen Physiol 90:229–259

Sakuranaga M, Sato S, Hida E, Naka K-I (1986) Nonlinear analysis: mathematical theory and biological applications. CRC Crit Rev Biomed Eng 14:127–184

Wiener N (1958) Nonlinear problems in random theory. Wiley, New York

Zohar S (1979) Fortran subroutines for the solution of Toeplitz sets of linear equations. IEEE Trans ASSP-27:656–658

Received: August 20, 1987

M. J. Korenberg
A. S. French
S.K.L. Voo
Department of Electrical Engineering
Queen's University
Kingston, Ontario
K7L 3N6 Canada
and
Department of Physiology
University of Alberta
Edmonton, Alberta
T6G 2H7 Canada